Projection display throughput: Efficiency of optical transmission and light-source collection

by F. E. Doany R. N. Singh A. E. Rosenbluth G. L.-T. Chiu

The optical system for a projection display based on three miniature reflective spatial light modulators (SLMs) is described. The total projection display light throughput is a function not only of the optical system efficiency but also of the light-collection and light-coupling efficiency referred to here as the lamp-SLM coupling. The optical system efficiency is the transmission of the optical components in the projection display. These are examined in detail through measurements and estimates of the components in the system. The various optical components include UV-IR filtering, illumination optics, polarization optics, color separation and recombination optics, SLM efficiency, and projection optics. The lamp-SLM coupling, which is the amount of usable light that can be collected from a particular lamp coupled to

the projection optical system, is determined by the light-source luminance, the efficiency of the light-collection optics, and the optical system étendue. For small SLMs, less than 50 mm diagonal, for example, the lamp-SLM coupling efficiency falls off rapidly with SLM size and optical system f-number. The dependence of this coupling efficiency on SLM size is determined from measurements of the light-collection efficiency as a function of aperture size, where the apertures are used to simulate SLMs of the same dimensions. A variety of arc lamps were investigated for use in the projection display based on IBM reflective SLM devices. The lamp-SLM coupling dependence on arc gap was determined. The measurements are used to compare various lamps and to estimate directly the throughput for the complete

Copyright 1998 by International Business Machines Corporation. Copying in printed form for private use is permitted without payment of royalty provided that (1) each reproduction is done without alteration and (2) the Journal reference and IBM copyright notice are included on the first page. The title and abstract, but no other portions, of this paper may be copied or distributed royalty free without further permission by computer-based and other information-service systems. Permission to republish any other portion of this paper must be obtained from the Editor.

0018-8646/98/\$5.00 © 1998 IBM

projection system. The SLMs used in the projection display are liquid crystal devices which utilize only one polarization of light while discarding the second. Converting the discarded polarization into useful light can in principle double the throughput of the projector. However, polarization conversion results in doubling of the size of the light source and thus produces less efficient lamp—SLM coupling, particularly for long-arcgap lamps. Measurements and analysis of throughput enhancement by polarization conversion are presented, and the dependence on arc gap and optical system étendue is discussed.

Introduction

The total light output of projection displays employing a light source that illuminates spatial light modulators (SLMs) is a function of the efficiency not only of the projection optical system but also of the light collection and light coupling. In projectors using large spatial light modulators, the emphasis on projector throughput analysis and throughput enhancement has been on the transmission efficiency of the optical components. The total system throughput also includes the light-coupling efficiency. For a small SLM diagonal $(D_{SLM})^{1}$ for example less than 50 mm in length, the efficiency of coupling the lamp light to the SLM (referred to as the lamp-SLM coupling efficiency) falls off rapidly with light-source arc length and projection optics f-number, where the f-number is the customary expression of the ratio of the focal length of a lens to the diameter of the incoming beam. Recent advances in SLM technology have resulted in highresolution spatial light modulators with $D_{\rm SLM}$ in the 0.5-1.3-in. range, where the smallest D_{SLM} are predominantly based on crystalline silicon devices such as the IBM liquid crystal SLM devices described in this issue, the Texas Instruments digital mirror devices (DMDs) [1], and the Pioneer liquid crystal SLM devices [2]. For projectors using such devices, the lamp-SLM coupling efficiency can become the dominant factor limiting the light output.

Transmission liquid crystal SLMs using polysilicon device technology are also in the 1.3-in. $D_{\rm SLM}$ range and possess similar throughput limitations, though they are not as severe. Projectors using transmissive devices can operate at smaller f-numbers, allowing greater light-collection efficiency. Extension of the p-Si technology to smaller, higher-resolution SLMs (i.e., having greater pixel

Optical throughput of the projection system

The total projector light throughput is the amount of light delivered by the optical projection system to the viewing screen and is measured as the total light flux, F, in units of lumens. Three parameters contribute to limiting the total light flux. The first, the optical transmission factor (T_{ox}) , results from losses introduced by all of the optical components in the total system light path, including polarization and spectral filtering losses. Another is the brightness of the light source, or its luminance B_s , which is measured in units of lumens/sr-m² (or cd/m²). Finally, the light flux is restricted by the product of the lightacceptance solid angle and the area of the limiting aperture in the projection optical system. This quantity is known as the étendue (E), or "optical extent," of the system and is measured in units of sr-m². For typical projection systems using small SLMs, the limiting aperture is the size of the SLM, and the solid acceptance angle is derived from the f-number. The projection system's light flux F_p , in lumens, is given [3] by

$$F_{p} = B_{s} \cdot E \cdot T_{os} \,. \tag{1}$$

For our specific application of projection systems, an arc lamp typically encased in an integral parabolic or ellipsoidal reflector currently available from vendors is used to provide maximum arc/reflector alignment efficiency. For convenience in the analysis of the projection system throughput, the luminance $B_{\rm s}$ of the light source is assumed to include brightness-limiting effects due to the lamp reflector as well as the arc lamp itself. This allows the separation of lamp-related contributions from optical-system contributions. Thus, for a specific lamp, the effective light-source luminance is a function of the arc-lamp properties (lamp power, arc size, luminous efficacy, and distortion due to the bulb envelope) and the reflector properties (geometric efficiency of the reflector, optical coatings efficiency of

density) is limited because of the diminishing area available per pixel for a clear aperture required for light transmission. Thus, high-resolution projectors will rely on crystalline silicon device technologies, which are predominantly reflective devices. As described below, optical projection systems based on reflective SLMs require limited optical system acceptance angles (or f-numbers), thus limiting light-collection efficiency. This paper concentrates on an analysis of light throughput of projectors using reflective SLM devices. In addition to analysis of the optical system efficiency, the lamp-SLM coupling efficiency is studied as a function of light-source arc gap and optical system acceptance angle. The dependence of the total system throughput on the key optical and lamp parameters is discussed, and requirements for optimum performance are established.

¹ The size of a spatial light modulator (SLM) is described by the length of its diagonal.

² The length of D_{SLM} for SLMs is typically given in inches.

the reflector, and distortion due to the optical quality of the reflector). These factors together define the effective light-source luminance, B_{lamn} , which includes the lamp/reflector étendue. For a system designed for maximum efficiency, this étendue should match the étendue of the projection system.

In the case of projectors using small SLMs, the aperture limiting the optical system is the size of the SLM. The acceptance solid angle is proportional to the square of the numerical aperture $(NA)^2$ of the optical system, where $NA \equiv n \sin \theta \simeq 1/2 (f-number)$ and n(air) = 1 is assumed. In terms of $D_{\rm SLM}$, rather than SLM area, the étendue is proportional to $(D_{SLM} \cdot NA)^2$. The product $(D_{\text{SLM}} \cdot NA)$ is a measure of the optics-SLM system acceptance, which determines the projector's final throughput of light. To increase the throughput (by increasing the system's acceptance), the NA must be increased and/or the SLM size must be increased. However, the trend is to decrease the size of the SLM in order to lower cost. The numerical aperture can be increased to some extent, but not without a penalty. Reflective SLM operation demands stringent requirements of the optical system for color separation/recombination and for polarization control of the incoming and exiting light bundles. The difficulty in meeting these requirements increases dramatically at high NA. The liquid crystal (LC) contrast ratio can also degrade at high NA, depending on the LC mode of operation. Specific values of NA and SLM size and their impact on throughput are discussed below. A projector employing reflective SLMs must therefore be optimized for NA, SLM size, and light-source luminance.

To simplify the analysis of projection optical systems, the lamp parameters are separated from the optical-system parameters. The light-source luminance is replaced by the effective lamp luminance, B_{lamp} , which includes brightnesslimiting factors due to the reflector (geometrical efficiency, reflectivity, and optical aberrations). Rewriting Equation (1) in terms of lamp and NA parameters gives

$$F_{\rm p} = B_{\rm lamp} \cdot \frac{\pi}{2} \left(D_{\rm SLM} \cdot NA \right)^2 \cdot T_{\rm os} \,. \tag{2}$$

The effective lamp luminance, B_{lamp} , and the optics-SLM acceptance, $(D_{\text{SLM}} \cdot NA)^2$, determine the total usable lumens collected from a specific lamp by an optical system with a specified NA and SLM size. This usable light, F_{lamp} , is a measure of the lamp-SLM coupling efficiency, and is given by

$$F_{\text{lamp}} = B_{\text{lamp}} \cdot (D_{\text{SLM}} \cdot NA)^2. \tag{3}$$

 F_{lamp} can be measured directly for each lamp as a function of $\dot{N}A$ and $D_{\rm SLM}$, thereby allowing a direct lamp-to-lamp comparison of the final projector output. Implicit in

Equation (3) is that the étendue is limited by the optical system—the point at which the light collected is much less than the total lamp output; i.e., $F_{\text{lamp}} \ll F_{\text{max}}$. However, as $(NA \cdot D_{SLM})^2$ becomes large compared to the lamp/reflector étendue, the total lamp output, F_{max} , is collected by the optical system. Between these two limits, the collected light is a function of both $NA \cdot D_{SIM}$ and the lamp/reflector étendue E_0 . These three regions are

$$F_{\text{lamp}} \propto (NA \cdot D_{\text{SLM}})^2$$
 for small $(NA \cdot D_{\text{SLM}})$; (4a)

$$F_{\text{lamp}} = F[(NA \cdot D_{\text{SLM}}), E_0]$$
 for intermediate-size $(NA \cdot D_{\text{SLM}});$ (4b)

$$F_{\text{lamp}} = F_{\text{max}}$$
 for large $(NA \cdot D_{\text{SLM}})$. (4c)

An approximate general expression for F_{lamp} , based on a model of the lamp/reflector étendue-limiting parameters, is derived in [4]:

$$F_{\text{lamp}}(d) = F_{\text{max}} \cdot L(D_0, Z_0, f, d),$$
 (5)

where F_{max} is the total arc lamp/reflector light flux which includes the reflector coating and geometric efficiencies. L is a function of the arc diameter (D_0) and length (Z_0) , arc intensity distribution f, and the parameter d, which depends on the optical system étendue, an ideal (cylindrical) arc étendue, and a parameter corresponding to the reflector aberrations. Specifically, d is proportional to the ratio of the optical system étendue to the lightbeam étendue E_0 ; i.e., $d \propto (NA \cdot D_{SLM})^2 / E_0$. The algebraic derivation obtained from this model does not lead to a closed analytical solution; it requires a specific lamp/reflector model and it has several approximations, but it is useful if the arc and reflector parameters are known. In general, however, this information is not available for every lamp/reflector combination. In the limit of optical system étendue >> lamp/reflector étendue, the value of F_{lamp} given by Equation (5) becomes a constant

For each lamp, the final projector output, F_n , is determined by the product of the optical system efficiency and the usable light flux collected by the system, and is

$$F_{p} = F_{lamp}[(NA \cdot D_{SLM}), E_{0}] \times T_{os}$$

$$= I_{sum} SLM \text{ sometime } \times \text{ antical effection } (6)$$

 $\equiv lamp-SLM \ coupling \times optical \ efficiency.$

This analysis separates the lamp-related parameters from the optical-system transmission. For a specific lamp/reflector combination (with constant E_0), the dependence of F_{lamp} on NA and D_{SLM} can be measured directly. This allows measurement of the total number of usable lumens from any lamp/reflector, for all values of $D_{\text{SIM}} \cdot NA$. The following sections describe in detail the prototype projection display based on IBM reflection

389

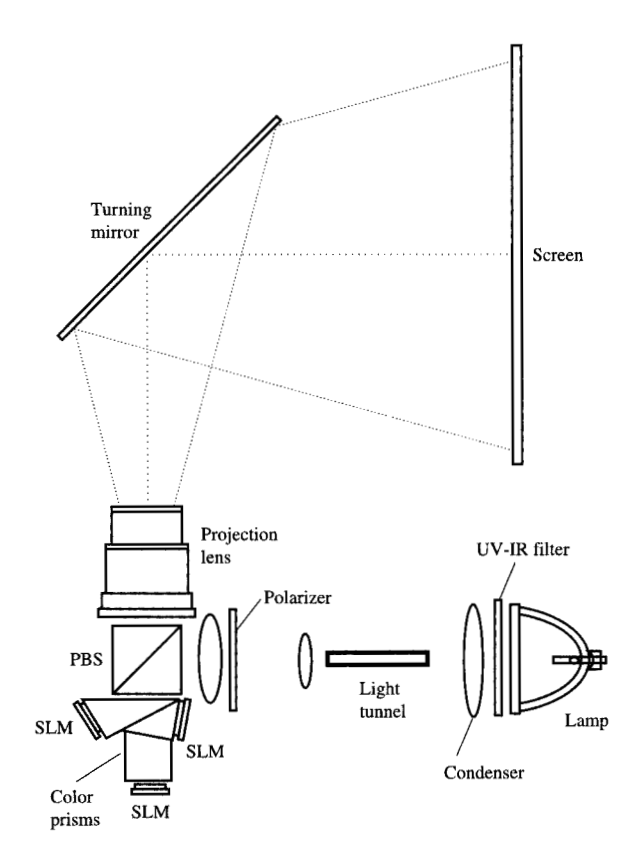


Figure 1

Optical system of high-resolution projection display using reflective SLMs.

SLM technology, the measurements of the optical system efficiency, and the measurements and modeling of the lamp-SLM coupling.

Prototype high-resolution projection display

A prototype high-resolution desktop projection display with data, graphics, and video capability was designed, built, and evaluated [5]. A schematic drawing of the projection display using three liquid crystal reflective SLMs is shown in **Figure 1** (see papers in this issue for further details). The SLM used in the prototype system has a 1.94-in. diagonal, and the array contains 2048×2048 square-shaped mirrors on a 17- μ m pitch. The illumination system consists of an arc lamp in a parabolic reflector. After UV (ultraviolet) and IR (infrared) filtering, the white-light source is focused into a light tunnel to homogenize the light. The uniform output of the light tunnel is collected and imaged onto the three SLMs through the polarization and color separation optical assembly. This optical assembly consists of a polarizing

beam-splitter (PBS) cube and a three-prism color-splitting assembly. The polarizing cube directs one polarization (S) toward the SLMs and discards the opposite (P) polarization. The color three-prism assembly separates white light into red (R), green (G), and blue (B) components and directs each component to its respective SLM. The SLMs function by selectively rotating the incoming polarization from S- to P-polarization on a pixelby-pixel level and reflecting the light back to the color prism assembly. The light retraces its path through the color prism assembly, which recombines the R, G, and B light into the composite white light. The PBS then discards the S-polarized light by reflecting it back toward the illumination and directs the P-polarized image-forming light to the projection lens, which magnifies and images the full-color composite image onto the screen.

The final embodiment of the prototype system is a high-resolution rear-projection monitor. The image size on the screen is 20 in. \times 20 in. At this magnification, the pixel size on the screen is 0.25 mm. The resulting screen resolution is \sim 100 pixels/in. over the entire 28-in.-diagonal image of the >4-megapixel display. The measured screen luminance from the 100-W arc-lamp illumination source is about 100 cd/m².

Efficiency of the optical system

The optical system efficiency, or transmission factor $(T_{\rm os})$, is examined in detail from measurements and estimates of all optical components in the projection system. The optical components include UV-IR filtering, illumination optics, polarization optics, color separation optics, SLM efficiency, color recombination optics, and projection optics. The system also includes contrast and/or colorenhancement components, and a screen for rear-projection displays.

The overall throughput of the prototype system was limited by the design NA and the efficiencies of the optical components. In designing the prototype projector depicted in Figure 1, the optical system f-number was f/5 (0.10 NA). Several factors contributed to this choice, including the performance of the polarizing beamsplitter coating and dichroic color-splitting coatings, and compound-angle depolarization effects. Spectral filtering was accomplished in several stages: by two UV-IR filters, two dichroic coatings at the interfaces of the three-prism color assembly used in double-pass mode for splitting and combining, and absorbing color filters at the SLMs. These were adopted to provide saturated and balanced colors. The illumination system is based on a light-tunnel homogenizer comprising a hollow mirror tunnel fabricated using aluminum mirrors. The illumination system also included several optical elements and aluminum turning mirrors limiting the overall efficiency. Table 1 presents a summary of the optical components in the prototype

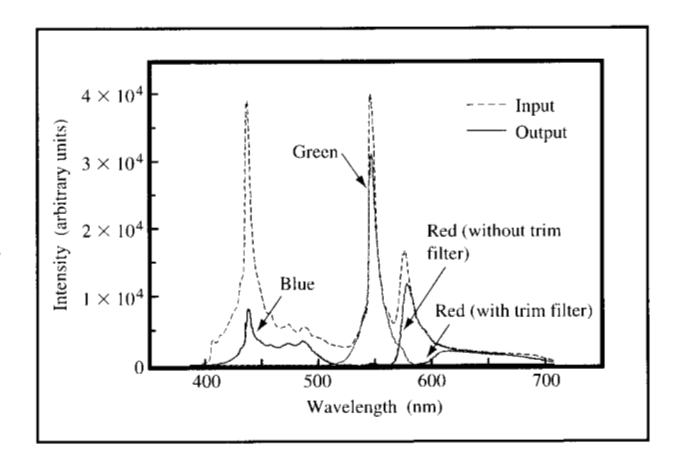
system and their measured or estimated efficiencies. The optical components are divided into six subsystems of the overall projection system: 1) ultraviolet and infrared filters, 2) illumination optics, 3) polarization optics, 4) spectral filtering optics, 5) projection optics, and 6) SLMs.

As shown in Table 1, the final optical system efficiency is $\sim 2.5\%$. Using 3600 lumens as the total usable lumens collected from the lamp (see below), this optical efficiency results in 90 lumens incident on the screen. The prototype system is set up as a rear-projection monitor. Surface-diffusing screens with a low gain (of order 1.5–2) were selected to provide wide viewing angles and maintain high resolution on the screen. For additional discrimination against room light, a gray (absorbing) screen with a gain of 2 was favored. The resulting net rear-projection system screen luminance was 115 cd/m².

Table 1 also shows that the estimated optical-system efficiency that could be realized in an improved system is in the 9-10% range. This $\sim 4 \times$ gain in optical transmission is not the result of a single specific improvement. As shown in Table 1, improvements in each of the six subsystems are necessary to realize this optimum transmission efficiency. Measurements and estimates were conducted to analyze the losses and determine the potential gain in all six subsystems listed in Table 1. For example, the greatest gain can be realized by improving the spectral efficiency of the total optical system. This is clearly illustrated in Figure 2, which shows the input lamp spectrum and the spectrum of the projector output measured at the screen. Substantial losses in most subsystems at the extremes of the spectrum limited the total spectral efficiency, particularly losses in the blue. An attenuation (~40%) of the green channel was required for a balanced white point.

Experimental measurements of lamp-SLM coupling

As described above and given in Equations (3)–(5), the lamp-SLM coupling efficiency F_{lamp} is a function of NA, D_{SLM} , and lamp/reflector étendue (E_0) , and determines the amount of usable light that is collected from a lamp. For a specific lamp/reflector (with fixed E_0), the amount of usable light flux can be determined directly from measurements of the light throughput through an aperture. The measurement apparatus is shown in Figure 3. For lamps in parabolic reflectors, the UV and IR are first filtered from the light output. The light is then typically focused by a condenser lens at 0.25 NA into a variable aperture. A second fixed aperture at the condenser lens is used to provide a well-defined NA. The total optical power transmitted through the variable aperture is then recorded as a function of aperture size. For lamps provided with an ellipsoidal reflector, the light is usually collimated and then measured using the same



Emilia 2

Input lamp spectrum and the output spectra from the three individual R, G, B channels. The red output spectrum is shown with and without a trim filter used to obtain proper color balance.

Table 1 Optical transmission efficiency of the subsystems of the prototype projection display.

| | | Prototype system | Improved efficiency |
|---------------------------------------------------|------|---------------------|---------------------|
| UV-IR filter | | 0.86 | 0.90 |
| Hot mirror* | 0.9 | | |
| $Cold\ mirror^{\dagger}$ | 0.95 | | |
| Illuminator | | 0.65 | 0.85 |
| Homogenizer | 0.85 | | |
| Lenses | 0.94 | | |
| Mirrors | 0.81 | | |
| Polarization | | 0.36 | 0.38 |
| Pre-polarizer | 0.42 | | |
| PBS [§] (two-pass) | 0.88 | | |
| $\lambda/4$ (contrast filter) | 0.98 | | |
| Spectral efficiency | | 0.38 | 0.6 - 0.7 |
| Color prisms: | | | |
| Dichroics/surfaces | 0.75 | | |
| Color filtering: | | | |
| Filter (yellow) | 0.85 | | |
| Color balance | 0.6 | | |
| Projection system | | 0.81 | 0.90 |
| Lens | 0.9 | | |
| Turning mirror | 0.9 | | |
| SLM | | 0.40 | 0.55-0.6 |
| Optical system transmission efficiency (T_{os}) | | 0.025 | 0.081-0.10 |

^{*}Hot mirror is IR-transmitting/visible-reflecting.

system. In addition to the above data, the total power emitted by the lamp/reflector is measured by replacing the

condenser with a high-NA lens and focusing the light into

[†]Cold mirror is visible-reflecting/IR-transmitting. §PBS is the polarizing beam-splitter cube.

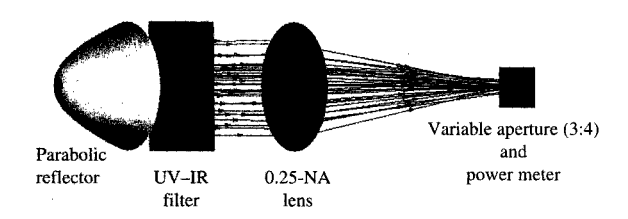


Figure 3

Schematic of lamp measurement apparatus. The visible output of a lamp/reflector is first filtered of UV-IR light and then focused at 0.25 NA into variable apertures. The apertures are rectangular, with a length ratio of 3:4, simulating the SLM aspect ratio. The energy transmitted by the apertures is detected using a power meter.

a detector. This measurement provides the maximum light flux that can be collected from the lamp/reflector (F_{max}) .

The recorded power is then corrected for component losses (UV-IR filter and lenses). The light power is measured using a power meter in units of W. Spectral analysis of the light transmitted through the UV-IR filters leads to a conversion factor from W to lumens. For example, the conversion factor is determined as 300 lumens/W for the Philips UHP-100W lamp [6] and 230 lumens/W for the ILC Cermax Xe arc lamp [7]. For direct comparison to SLMs, the experimental apertures used to simulate SLMs are typically rectangular, with 3:4 length ratio, and are designated by their diagonal length, $D_{\rm SLM}$.

The direct measurement gives the amount of usable light flux as a function of $D_{\rm SLM}$ at 0.25 NA. Though collected at 0.25 NA, the data can be used to determine the expected light flux at any NA. In a well-corrected optical system, the étendue is preserved and $NA \cdot D_{\rm SLM}$ is constant. Since the aperture can be imaged onto the SLM at arbitrary magnification, the resulting NA at the SLM is simply the input NA (0.25) divided by the magnification factor. Similarly, the resulting equivalent $D_{\rm SLM}$ is the product of the input diagonal and the magnification factor. For example, the light flux at 0.25 NA through apertures of one-half the diagonal.

A variety of arc lamps were investigated for use in the projection display based on IBM reflective SLM technology. Data for two lamps with very short arc gaps are presented in **Figure 4**. One lamp is the Philips UHP-100W lamp [6] with a 1.4-mm arc gap and a spectrum similar to that of a metal halide. The second is the ILC Cermax 500W Xe arc lamp [7] with a 1.15-mm arc gap. The 100-W lamp is housed in a parabolic reflector, and the 500-W lamp in an ellipsoidal reflector.

The plots presented in Figure 4 show the total usable lamp power (W) that can be collected at 0.25 NA for various aperture diagonals (3:4 rectangular aperture). Additional data collected for the 100-W lamp using square apertures show identical dependence. As seen in the data, the collected power increases rapidly for apertures with small diagonals, and begins to level off for diagonals greater than 20 mm.

The maximum usable light flux, $F_{\rm max}$, is also experimentally measured. The apparatus depicted in Figure 3 was modified by removing all apertures, using a high-NA lens to collect the total emitted lamp light, and focusing the light into the detector. The measured power collected (at high NA) from these two lamps is $\sim 18~{\rm W}$ and $\sim 43~{\rm W}$.

The experimental measurements show both the usable light flux at various apertures and the maximum usable light flux. The maximum usable light flux, $F_{\rm max}$, which includes the reflector collection efficiency (both geometric and coatings reflectivity), is typically much less than the total arc luminous flux, F_0 . The total luminous flux F_0 , the product of the lamp power (W) and the luminous efficacy (lumens/W), is specified by lamp manufacturers as the lamp output. However, the important quantity for projection system designers is not F_{0} but rather F_{max} . From the measurements of total usable light flux, most lamp/reflector combinations provide 40-50% of the total luminous flux supplied in the lamp specifications, or $F_{\rm max}/F_0 \sim 0.4-0.5$. The total usable flux must be measured rather than relying on the specification of total power (W) and luminous efficacy (lumens/W). Exceptional lamp/reflector efficiencies can be in the 60-70% range $(F_{max}/F_0 \sim 0.6-0.7)$. The total power emitted from the two lamps measured above is indicative of efficient reflectors, both in geometry and in coating reflectivity.

The saturation effect at large aperture diagonals is predicted by the analysis presented earlier. The analysis also predicts a quadratic dependence for small diagonals. The data depart from linear dependence only for very small (\ll 10 mm) aperture diagonals, although the exact dependence cannot be determined because of insufficient data at these dimensions. Only the region where the collected power is small (<20% of the maximum) shows a nonlinear dependence. This region of low collection efficiency is not of great interest in the design of projection optical systems. The intermediate region shows an approximately linear dependence on the size of aperture diagonals.

Modeling of lamp-SLM coupling

The dependence on aperture diagonal size leading to three regions of behavior (quadratic, near-linear, and saturation) for the collection efficiency is predicted by several models. The three-dimensional model of the arc and reflector leading to the full expression for F_{lamp} given in [4] exhibits this behavior. A phenomenological model predicting this behavior which also provides intuitive understanding of the data considers a two-dimensional image of the arc as having an inner core of constant brightness, B_s , followed by a radial brightness dependence proportional to 1/r which decreases to 0 at an outer radius. This arc intensity distribution leads directly (see the Appendix) to the light-flux dependence having three distinct regions: 1) a region of quadratic dependence on aperture diagonal size for small diagonals, 2) a region of linear dependence on aperture diagonal size for intermediate-size diagonals, and 3) a constant or saturated region corresponding to large aperture diagonals.

A more precise simulation of the measured dependence can be derived by computer modeling of the arc lamp. Such modeling requires input of the arc intensity distribution and the bulb envelope as well as the reflector geometry. Using such data, a ray-tracing simulation of the light collected and coupled into the SLM from the lamp-reflector combination was performed using ASAP [8] ray-tracing software. The ASAP software was able to provide the necessary modeling of the arc as an extended light source. Modeling of the 100-W lamp with the 1.4-mm arc gap was conducted for comparison to the measurements presented in Figure 4.

The lamp consisted of a bulb containing the arc, which was then mounted in a paraboloidal reflector. The geometries of the bulb and the reflector were modeled as optical refracting and reflecting surfaces. The arc was modeled using embedded volume emitters of suitable shape and size and positioned along the arc gap and apodized to simulate the radiation pattern of the lamp. Several thousand rays generated randomly from the emitters were propagated through the bulb and reflected by the reflector, resulting in a collimated beam of finite divergence. This beam was then focused onto a receiver with a lens operating at the NA of 0.25, as in the experimental measurements leading to the results presented in Figure 4. The receiver was rectangular, with a 3:4 aspect ratio, and was characterized by its diagonal.

A plot of the collected flux versus the diagonal of the aperture as computed by ASAP is shown in **Figure 5** for the UHP-100W lamp with the 1.4-mm arc gap together with the measurements from Figure 4. The model and measurements show excellent agreement. This verification constitutes a foundation for using the model and the measurements in the design of the illuminator for the projection display.

Examples of projector throughput estimates

For the specific case of the prototype projection display, the 100-W lamp illuminated the 49-mm-diagonal SLM using an optical system operating at 0.10 NA. Although

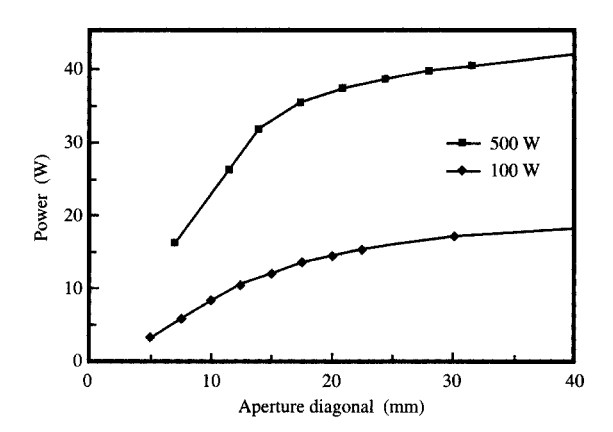


Figure 4

Lamp throughput vs. aperture diagonal measured at 0.25 NA for the UHP-100W 1.4-mm arc-gap and the Cermax 500W 1.15-mm arc-gap lamps.

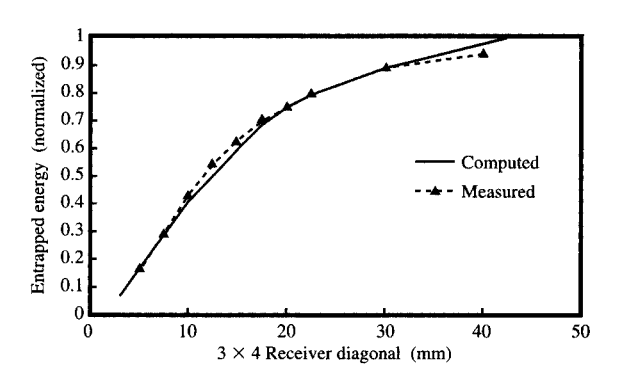


Figure 5

Comparison of simulated and measured throughput of the UHP-100W lamp. The simulation was calculated using the ASAP program. Both data curves are normalized to maximum output.

data are available for the square apertures, the collected light power is also determined from data in Figure 4, since there is only a 2% difference in diagonal between square and rectangular 3:4 apertures with equal areas. Since $NA \cdot D_{\rm SLM}$ is constant, an equivalent throughput parameter is 19 mm $D_{\rm SLM}$ at 0.25 NA. Figure 4 predicts that the total power usable by the optical system is 14 W. The actual power in the prototype system measured slightly lower at 12 W. The ~15% loss in collection efficiency is a result of two factors: 1) The structured, rather than smooth, parabolic reflector degraded the light divergence, and

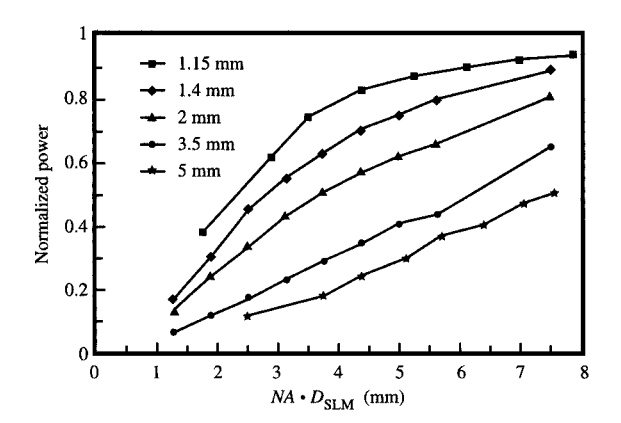


Figure 6

Comparison of throughput of five lamps with varying arc gaps. The throughput is normalized to maximum output for each lamp and is plotted against $NA \cdot D_{SLM}$.

2) the large separation of the lamp and the condenser lens due to optomechanical constraints also degraded the collection efficiency.

Finally, use of the conversion factor of 300 lumens/W shows the total usable light flux for the prototype projection display to be 3600 lumens. Use of the optical transmission factor of 2.5% shows a total of 90 lumens reaching the screen. The luminous flux at the 20-in. \times 20-in. screen is about 350 lumens/m². For the high-contrast gray screen with \sim 0.5 transmission and gain of 2, the resulting luminance is about 115 cd/m². This value is in close agreement with the measured screen luminance.

The lamp-measurement results can be used to compare various lamps and to directly estimate the throughput for the complete projection system. Although measured at 0.25 NA using the apparatus depicted in Figure 3, the results can be used to estimate the total projector throughput for any SLM diagonal and optical system NA. For example, consider a projection optical system operating at 0.125 NA. Use of an example of a typical SLM diagonal of 33 mm (1.3 in.) shows the equivalent diagonal at 0.25 NA to be 16.5 mm. At this diagonal, Figure 4 predicts the usable lamp power as 13 W from the 100-W lamp and 34 W from the 500-W lamp. Use of the conversion factors 300 and 230 lumens/W shows the usable lamp flux to be about 3900 and 8000 lumens for the two lamps, respectively. A projection system with about 9% efficiency would therefore result in an output of about 350 and 700 lumens from these two lamps.

In general, the throughput of a projector with a specified NA and SLM diagonal can be predicted, since $(NA \cdot D_{\text{SLM}})$ is a constant. To facilitate such prediction,

the data can be replotted as a function of $(NA \cdot D_{\rm SLM})$, rather than $D_{\rm SLM}$ at the specific measurement NA. This allows a direct determination of the total number of usable lumens for any projector with the specified NA and SLM diagonal.

The lamp-measurement procedure described above was carried out for a wide variety of arc lamps considered for projection applications. As expected, lamps with shorter arc gaps allowed greater collection efficiency. In the example given above, 72% and 79% of the total lamp output is collected from the two lamps with 1.4-mm and 1.15-mm arc gaps, respectively. The lamp-SLM arc-gap dependence can be examined in greater detail using the results of throughput vs. aperture diagonal for various lamps. Determination of the effect of the arc gap on collection efficiency is facilitated by normalization of the measured data. The measured power can be normalized to the maximum measured power, F_{max} (total power measured at high NA). Figure 6 shows this efficiency (relative to maximum lamp output) for several lamps with arc gaps of 1.15, 1.4, 2.0, 3.5, and 5 mm. For more general applications, the normalized power is presented as a function of $(NA \cdot D_{SLM})$, rather than D_{SLM} at 0.25 NA, where D_{SLM} is measured in units of mm.

As a reference point, the above example using 1.3-in. $D_{\rm SLM}$ at 0.125 NA corresponds to 4.1 mm on the $(NA \cdot D_{\rm SLM})$ scale. At this point, it is evident that the collection efficiency for the 3.5-mm and 5-mm arc gaps falls to 35% and 22%, respectively. Even for the 2-mm-arc-gap lamp, less than half the emitted power is collected by the optical system $(NA \cdot D_{\rm SLM} = 4.1 \text{ mm})$.

Polarization conversion for throughput enhancement

An important technique for increasing the system throughput is through polarization conversion. The IBM projection display prototype utilizes only one polarization for operation, while discarding the second. Converting the discarded polarization to the useful polarization can, in principle, double the throughput. However, polarization conversion results in doubling the apparent size of the light source and thus may result in less efficient lamp–SLM coupling.

Polarization conversion involves the following procedure. A polarizing beam-splitter (PBS) cube is used to separate the two polarization states. This produces two sources of light. A half-wave retardation plate (HWP) is placed in one beam of light, producing two sources of the same polarization. In a typical illumination system, both beams are subsequently used as the input source to the light homogenization system (e.g., light-tunnel or "fly's-eye" array). Since two beams are incident on the homogenization system, the size of the light source is effectively doubled.

In terms of polarization optical efficiency, a polarization-conversion system (PCS) can significantly improve light output. The polarized light output can be about 1.85 times greater with PCS than without it, with the only losses due to incomplete polarization control by the PBS and half-wave retardation plate (\sim 0.92 efficiency assumed).

Earlier polarization-conversion schemes, such as those described in [9, 10], accomplish the conversion in a collimated beam. Figure 7(a) shows a schematic of a PCS system operating in a collimated beam. An aperture limiting the transmission of the input beam is placed at the input to the PCS. In an optical system where $NA \cdot D_{\text{SLM}}$ is in the saturated region, all of the lamp light is transmitted through the limiting aperture, resulting in a highly efficient PCS. In this case, the optical system can accommodate a larger aperture, such as that produced by doubling of the light source. However, for the more typical case in which $NA \cdot D_{SIM}$ is not in the saturated region, the usable light flux transmitted by the limiting aperture is less than the maximum flux, since the light source is already overfilling the system acceptance $(NA \cdot D_{SLM})$. For an arc-lamp source that is collimated by a reflector (or other optics), the intensity in the beam is distributed throughout the entire beam. Since polarization conversion doubles the size of the beam, polarization conversion using a collimated beam produces marginal gain in the system throughput. Our initial measurements using a collimated beam for the prototype projector optical parameters ($NA \cdot D_{SLM} = 4.9 \text{ mm}$) indicated that an increase in throughput of only 32% would be realized by polarization conversion.

An alternative technique yielding higher efficiency uses polarization conversion at the focus, as described in [11]. To achieve maximum efficiency from polarization conversion, the doubling of the source must occur at the position where the intensity distribution is highly concentrated, not at the distributed intensity of the collimated beam. The maximum concentration of light is produced at the image of the arc source itself, e.g., at the focus of a lens placed in the collimated light beam. Figure 7(b) shows polarization-conversion optics designed to operate at the focus. The system takes advantage of the "hot spot" in the intensity distribution to produce the maximum efficiency. At the focus, the intensity transmitted by the limiting aperture is greater than that transmitted in a collimated beam. Another difference shown in Figure 7(b) is that the input beam is divided into multiple smaller beams using a fly's-eye lens array. For the PCS, this allows a more compact system.

The gain that can be achieved using polarization conversion at the focus can be estimated from the lamp measurements presented above. The lamp data in Figures 4 and 6 show the usable light flux for $NA \cdot D_{\rm SLM}$ values. To estimate the gain, consider an aperture with diagonal

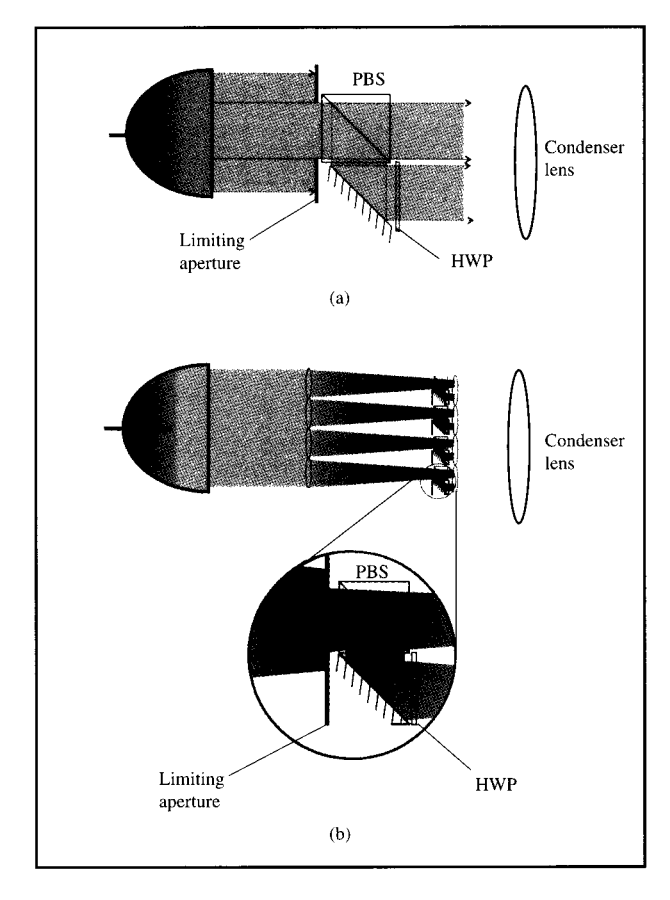
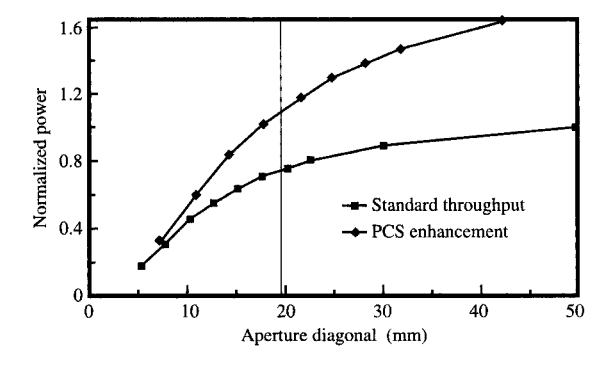


Figure 7

Comparison of polarization conversion systems (PCS): (a) Schematic of PCS using the collimated light beam. (b) PCS operating at the focus of the beam. The focused-beam PCS is shown with multiple focused sub-beams (as described in [11]), with an insert showing a magnified image of one of the sub-beams with a hot spot (red).

 $D_{\scriptscriptstyle \mathrm{SLM}}$. Figure 4 gives the usable light flux at diagonal $D_{\scriptscriptstyle \mathrm{SLM}}$ (and 0.25 NA) without polarization conversion. A PCS system requires one-half the area for the original beam, reserving the other half for the "converted" beam. For a PCS, the usable light flux from the lamp is therefore that light which is collected into an aperture with one-half the area of the original aperture of diagonal $D_{\rm SLM}$. Since the exact shape of the aperture is unimportant (to first order), an aperture with one-half the area is one of the same shape but diagonal $D_{SLM}/\sqrt{2}$. By using Figure 4, the usable light flux at $D_{\text{SLM}}/\sqrt{2}$ is determined directly. This measurement is available for all apertures (i.e., all $NA \cdot D_{\text{SLM}}$ values). As estimated above, the polarized light output of the PCS can be 1.85 times greater than a conventional (non-PCS) system. The conventional usable light flux through an aperture with diagonal D_{SLM} is



a a fail line i

Throughput of the UHP-100W lamp, normalized to maximum output, compared to the estimated enhanced throughput obtained using PCS with a focused beam.

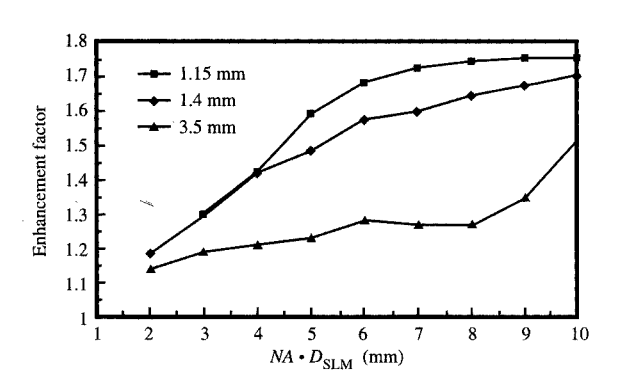


Figure 9

Ratio of throughput obtained using a focused-beam PCS to throughput obtained without a PCS. This PCS enhancement ratio is shown for lamps with three arc gaps: 1.15, 1.4, and 3.5 mm.

 $F_{\rm lamp}(D_{\rm SLM})$, and can be measured directly from Figure 4. From the above analysis, a PCS provides a usable light flux through an aperture with diagonal $D_{\rm SLM}$ equivalent to

$$F_{\text{PCS}}(D_{\text{SLM}}) = 1.85 \cdot F_{\text{lamp}}(D_{\text{SLM}}/\sqrt{2}).$$
 (7)

An example of using Equation (7) to determine the throughput enhancement that results from PCS at the focus is shown in **Figure 8**. Figure 8 presents the original data of Figure 4 for the UHP-100W lamp, normalized to the maximum measured power, as well as the estimated throughput of the PCS according to Equation (7). Using the optical parameters for the prototype display (49-mm

 $D_{\rm SLM}$ at 0.1 NA is equivalent to 19.6-mm $D_{\rm SLM}$ at 0.25 NA), Figure 8 gives the throughput without the PCS as 0.75, while the throughput including the PCS is estimated to increase to 1.10. This is a throughput-enhancement factor, or PCS efficiency, of 1.47 compared to only 1.32 for the earlier case of PCS using a collimated beam. Similarly, using the previous example of a 1.3-in.-diagonal aperture at 0.125 NA, Figure 8 estimates the throughput enhancement using the PCS at 1.42. It is evident from Figure 8 that the PCS efficiency is very limited for apertures of less than 12-mm $D_{\rm SLM}$ and becomes quite significant for apertures greater than 15-mm $D_{\rm SLM}$ (at 0.25 NA).

As described above, the polarization-conversion efficiency ξ_{PCS} is the ratio of the usable light flux with and without the PCS, given by

$$\xi_{\text{PCS}}(D_{\text{SLM}}) = \frac{1.85 \cdot F_{\text{lamp}}(D_{\text{SLM}}/\sqrt{2})}{F_{\text{lamp}}(D_{\text{SLM}})}.$$
 (8)

In a more general description, the dependence of $F_{\rm lamp}(D_{\rm SLM})$ on $D_{\rm SLM}$ can be replaced by the dependence on $NA \cdot D_{\rm SLM}[F_{\rm lamp}(NA \cdot D_{\rm SLM})]$.

By using the original lamp throughput data, such as that given in Figure 4, the polarization-recycling efficiency is calculated for any lamp and any optical system with a specified $NA \cdot D_{SLM}$. Figure 9 presents the polarizationconversion efficiency for the two lamps shown in Figure 4, which have arc gaps of 1.15 mm and 1.4 mm. As is evident in Figure 9, the PCS efficiency approaches 1.85 only for large values of NA \cdot $D_{\rm SLM}.$ For small NA \cdot $D_{\rm SLM}$ values, the PCS efficiency is low at <1.25. For these two lamps, the PCS efficiency increases dramatically for $NA \cdot D_{SIM}$ values greater than 2.5 mm. In the specific example used earlier of $NA \cdot D_{SIM} = 4.1 \text{ mm}$ (1.3-in. D_{SIM} at 0.125 NA), the PCS efficiency of both of these two lamps is ~ 1.4 . Figure 9 also presents the PCS efficiency predicted for the lamp with the 3.5-mm arc gap. For this lamp, Figure 6 shows that less than 35% of the total light flux is usable. The PCS analysis also estimates that the PCS efficiency for this example is only 1.2. In general, for this relatively large arc gap of 3.5 mm, the PCS efficiency does not show a substantial increase except for $NA \cdot D_{SLM} > 8$ mm.

In the example above, $NA \cdot D_{\rm SLM} = 4.1$ mm. For typical projection systems using small diagonal SLMs (≤ 1.3 in.) and typical optical systems ranging from f/4 to f/2.5, the $NA \cdot D_{\rm SLM}$ values fall within the range of 1.5- \sim 6. It is evident from Figure 8 that only lamps with arc gaps less than 2 mm can provide substantial throughput enhancement by polarization conversion. Should SLM dimensions continue to decrease, the arc-gap requirement for an efficient PCS will also continue to decrease.

Finally, we can summarize the predicted throughput from a projection system using these two lamps. Assuming

Table 2 Estimated projector throughput for a 0.125-NA optical system using 1.3-in. D_{SLM} .

| Lamp | Arc gap (mm) | F _{max} , maximum lumens measured | Usable lumens (1.3-in. D _{SLM} , 0.125 NA) | Lumen output 9% optical system | PCS efficiency | Lumen output w/PCS |
|----------------------|--------------|-----------------------------------------------|--------------------------------------------------------|--------------------------------------|-------------------|-----------------------|
| UHP-100W arc lamp | 1.4 | 5400 | 3900 | 350 | 1.42 | 500 |
| 500W Xe arc lamp | 1.15 | 9900 | 7800 | 700 | 1,43 | 1000 |

an optical system transmission factor of 9%, **Table 2** presents the expected projector throughput.

Summary

An analysis of the total projection display system throughput has been carried out. The luminous flux produced by a projection system is determined by the optical transmission efficiency and by the lamp–SLM coupling efficiency. The optical transmission efficiency is determined from the losses due to all of the optical components in the system. The lamp–SLM coupling efficiency determines the usable light flux that can be collected from each lamp.

The optical transmission factor is evaluated by detailed measurements and analysis of the losses in all of the optical subsystem. The optical transmission efficiency of the prototype projection display was found to be 2.5%. However, we estimate for polarization-based liquid crystal SLMs, an optimized optical system may provide about 10% transmission.

A measurement methodology is outlined for determining the total usable lumens that can be collected from any lamp source by a projector's optical system. The usable light flux from a specific lamp is dependent on the optical system's numerical aperture and the SLM diagonal. Measurement of the lamp–SLM coupling efficiencies can be used to estimate the throughput of various lamps.

For small-diagonal SLMs less than 1.3 in. (33 mm) and typical projection-optics numerical apertures in the range of 0.125–0.2, long-arc-gap lamps provide very inefficient light-collection efficiency. Only lamps with arc gaps of less than 2 mm can provide greater than 50% light-collection efficiency, and the efficiency increases with decreasing arc gap. The projection system throughput can be substantially enhanced by using efficient polarization-conversion schemes. A method of estimating the polarization-conversion system (PCS) efficiency from the lamp measurements is presented. For throughput enhancement by polarization conversion, the arc-gap requirement is further reduced to ≤1.5 mm.

Appendix: Phenomenological model illustrating the three regions of lamp-SLM coupling dependence seen in the data

The light source is usually an arc lamp which has a "hot spot" at the center and falls off toward the edge. The two-dimensional optical image of the arc lamp serves as the source of the illuminator. One models the source brightness distribution N(r) by the expression

where r_0 is the radius of the central hot spot, and r_1 corresponds to an outer radius beyond which there is negligible light output. This concentric disc model is a reasonable approximation for the inner iso-brightness contours of a dc lamp or the image of a lamp/elliptical reflector combination. The amount of light flux F reaching the "detector" (SLM or power meter or screen) placed at a distance s as a function of NA, controlled by placing a variable-diameter aperture in front of the detector, is given by the expression

$$F = \frac{2N(r) \cdot A \cdot r \cdot dr \cdot \cos^4 \theta}{s^2},$$
 (10)

where $\tan \theta = r/s$, $\tan \theta_0 = r_0/s$, $\tan \theta_1 = r_1/s$, $dr = s \sec^2 \theta d\theta$, and A is the area of the detector. By substituting N(r) in the above and integrating with respect to the angle θ , we obtain

$$F = \pi B_s A \sin^2 \theta \qquad \text{for } r \le r_0,$$

$$F = \pi B_s A \cdot f(\theta) \qquad \text{for } r_0 < r \le r_1,$$

$$F = \pi B_s A \cdot f(\theta_1) \qquad \text{for } r_1 < r,$$
(11)

where

$$f(\theta) = \sin^2 \theta_0 + \tan \theta_0 \left[(\theta - \theta_0) + \left(\frac{\sin 2\theta - \sin 2\theta_0}{2} \right) \right]. \tag{12}$$

397

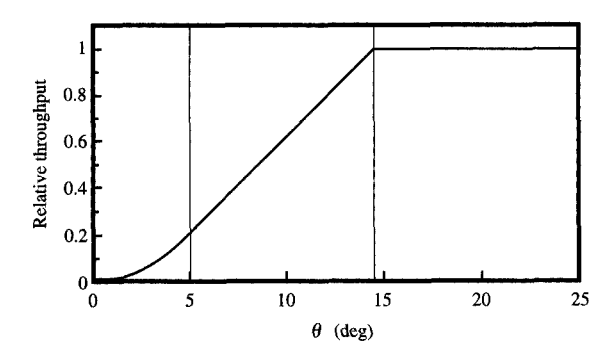


Figure 10

Throughput dependence derived from a phenomenological model described in the Appendix [Equations (10) and (11)]. At 0.25 NA, $\theta=5^{\circ}$ corresponds to $r_0=3.5$ mm, the radius of the inner constant-brightness region, and $\theta=14.5^{\circ}$ corresponds to $r_1=10$ mm, the outer radius beyond which the energy is negligible. These radii are equivalent to $D_{\rm SLM}$ values of 8.8 and 25 mm at 0.25 NA.

For a qualitative comparison to the data, consider an image of an arc at 0.25 NA with a 10-mm radius (r_1) and an inner hot spot of radius 3.5 mm (r_0) . Evaluating Equation (10) on the basis of these parameters leads to the result shown in Figure 10. Although Figure 10 gives the throughput dependence as a function of θ , the equivalent aperture diagonal can also be determined for a direct comparison with the data. For example, for $\theta = 5^{\circ}$ the corresponding 3:4 aperture diagonal is 8.8 mm, and for $\theta = 14.5^{\circ}$, the aperture diagonal is ~25 mm. Thus, a typical light source has three regions: for $r \le r_0$, we have a brightness-limited region where the light throughput has a quadratic dependence on NA; an intermediate region $r_0 < r \le r_1$, where the light throughput has a linear dependence on NA; and a lamp-limited region $r_1 < r_2$ where the light throughput is almost independent of NA.

Acknowledgment

The authors wish to acknowledge Hans van Wijngaarde for providing the UHP-100 lamps and for many useful discussions of arc-lamp technology.

References

- J. B. Sampsell, "An Overview of the Performance Envelope of Digital-Micromirror-Device-Based Projection Display Systems," *Digest of Technical Papers*, Society for Information Display International Symposium, 1994, pp. 669-672.
- F. Sato and Y. Yagi, "High Resolution and Bright LCD Projector with Reflective LCD Panels," *Digest of Technical Papers*, Society for Information Display International Symposium, 1997, pp. 997–1000.
- W. T. Welford and R. Winston, High Collection Nonimaging Optics, Academic Press, Inc., San Diego, 1989.

- M. S. Brennesholtz, "Light Collection Efficiency for Light Valve Projection Systems," *Projection Displays II*, *Proc.* SPIE 2650, 71-79 (1996).
- R. L. Melcher, P. M. Alt, D. B. Dove, T. M. Cipolla, E. G. Colgan, F. E. Doany, K. Enami, K. C. Ho, I. Lovas, C. Narayan, R. S. Olyha, Jr., C. G. Powell, A. E. Rosenbluth, J. L. Sanford, E. S. Schlig, R. N. Singh, T. Tomooka, M. Uda, and K. H. Yang, "Design and Fabrication of a Prototype Projection Data Monitor with High Information Content," IBM J. Res. Develop. 42, 321–338 (1998, this issue).
- E. Schnedler and H. van Wijngaarde, "Ultrahigh-Intensity Short-Arc Long-Life Lamp System," J. SID XXVI, 131-134 (1995).
- R. Roberts and W. Moloney, "Long-Lived Sealed Beam Xenon Short-Arc Lamps for Projection Display," J. SID XXVII, 771–773 (1996).
- 8. ASAP 5.1, Breault Research Organization, Inc., 6400 East Grant Rd., Tucson, AZ 85715.
- K. Kubota, M. Imai, S. Kaneko, Y. Tashiro, K. Mochizuki, M. Sakamoto, and T. Matsumoto, "High Resolution High Brightness Liquid Crystal Projector for Work Station," Projection Displays, Proc. SPIE 2407, 119-124 (1995).
- J. F. Goldenberg and J. D. Eskin, "Illumination System for an LCD Display System," U.S. Patent 4,913,529, 1990.
- Y. Itoh, J.-I. Nakamura, K. Yoneno, H. Kamakura, and N. Okamoto, "Ultra-High-Efficiency LC Projector Using a Polarized Light Illumination System," *Digest of Technical Papers*, Society for Information Display International Symposium, 1997, pp. 993–996.

Received April 25, 1997; accepted for publication March 3, 1998

Fuad E. Doany IBM Research Division, Thomas J. Watson Research Center, P.O. Box 218, Yorktown Heights, New York 10598 (doanv@us.ibm.com). Dr. Doany is a Research Staff Member in the Optical Systems group at the IBM Thomas J. Watson Research Center. He received a B.S. degree in chemistry from Haverford College in 1978 and a Ph.D. degree in physical chemistry from the University of Pennsylvania in 1984. Dr. Doany was a Postdoctoral Fellow at the California Institute of Technology from 1984 to 1985, working on ultrafast laser spectroscopy. He subsequently joined IBM at the Watson Research Center, where he worked on laser spectroscopy, laser material processing, and applied optics. His current research activity is in projection display technology. Dr. Doany has written many technical papers. holds more than 15 patents, and has received two Research Division Awards from IBM, in 1994 and 1996. He is a member of the Optical Society of America and the Society for Information Display.

courses in the areas mentioned above. He holds six U.S. patents, and has received an IBM Outstanding Technical Achievement Award and five IBM Invention Achievement Awards. Dr. Chiu is a member of the Society for Information Display, the International Astronomical Union, and the Institute of Electrical and Electronics Engineers.

Rama N. Singh IBM Research Division, Thomas J. Watson Research Center, P.O. Box 218, Yorktown Heights, New York 10598 (rnsingh@us.ibm.com). Dr. Singh received an M.S. degree in physics from Lucknow University, India, in 1964, a Diploma of the IIT, Delhi, in applied optics in 1966, a Diploma of the Imperial College, London, in applied optics in 1968, a Ph.D. in physics from the University of Reading in the U.K. in 1977, and an M.S. in computer science from Polytechnic University in 1995. Dr. Singh was a member of the faculty of physics at the Indian Institute of Technology, Delhi, until 1980, a Principal Scientist in the Microlithography Division at Perkin-Elmer from 1980 to 1988, and a Research Staff Member at the IBM Thomas J. Watson Research Center since 1988. His principal interests have been in optical design in the fields of photolithographic instrumentation and display technology.

Alan E. Rosenbluth IBM Research Division, Thomas J. Watson Research Center, P.O. Box 218, Yorktown Heights, New York 10598 (aerosen@us.ibm.com). Dr. Rosenbluth received the Ph.D. degree in optics from the University of Rochester in 1982 as a Hertz Foundation Fellow. He has been a Research Staff Member at the IBM Thomas J. Watson Research Center since 1982. His principal research activities have been in photolithographic instrumentation and processing, display technology, and thin-film optics.

George L.-T. Chiu IBM Research Division, Thomas J. Watson Research Center, P.O. Box 218, Yorktown Heights, New York 10598 (gchiu@us.ibm.com). Dr. Chiu is a Senior Manager in the Systems, Technology and Science Department at the IBM Thomas J. Watson Research Center. He received a B.S. degree in physics from the National Taiwan University in 1970, a Ph.D. degree in astrophysics from the University of California at Berkeley in 1978, and an M.S. degree in computer science from Polytechnic University in 1995. He joined IBM in 1980 after having been on the staff of Yale University. Dr. Chiu has worked on picosecond device and internal node characterization, laser beam and electron beam contactless testing techniques, functional testing of chips and packages, optical lithography, flat-panel displays, projection displays, miniature displays, and computer packaging. He has published numerous papers and delivered several short

[[Page 400 is blank]]